JOURNAL OF GEOPHYSICAL RESEARCH, VOL. 102, NO. B3, PAGES 5243–5250, MARCH 10, 1997

Stress wave attenuation in shock-damaged rock

Cangli Liu and Thomas J. Ahrens

Lindhurst Laboratory of Experimental Geophysics, Seismological Laboratory
California Institute of Technology, Pasadena

Abstract. The velocity and attenuation of ultrasonic stress waves in gabbroic rock samples (San Marcos, California) subjected to shock loading in the 2 GPa range were studied. From P wave velocity measurements we determined the damage parameter D_p and crack density ε of the samples and related these to the attenuation coefficient (quality factor) under dynamic strains of 2×10^{-7} and at a frequency of 2 MHz using the ultrasonic pulse-echo method. A fit to the data yields the P wave spatial attenuation coefficient at a frequency of 2 MHz, $\alpha_p(D_p) = 1.1 + 28.2D_p$ (decibels per centimeter). From the relation between the attenuation coefficient and quality factor, the quality factor Q is given by $Q^{-1} = 0.011(1+25.6D_p)(1-D_p)^{1/2}$. Using O'Connell-Budiansky theory relating crack density to velocity, the parameter in Walsh's theory was determined based on experimental data. An approximate method is also proposed to estimate the average half-length of cracks based on the attenuation measurements.

Introduction

Experimental measurements of attenuation of ultrasonic waves in various rocks have been carried out since the 1940s using different techniques over a wide frequency range [e.g., *Born*, 1941; *Nur and Simmons*, 1969; *Spetzler and Anderson*, 1968; *Johnston et al.*, 1978; *Toksoz et al.*, 1979; *Winkler and Nur*, 1982; *Murphy*, 1984]. Typical methods employed include the ultrasonic resonant bar [*Johnston and Toksoz*, 1980], the rise time of ultrasonic pulses [*Gladwin and Stacey*, 1974], the pulse-echo technique [*Papadakis et al.*, 1973] and an improved pulse-echo technique [*Winkler and Plona*, 1982]. The commonly used parameters for describing attenuation are the attenuation coefficient α and the quality factor Q. These quantities are related by

$$\frac{1}{Q} = \frac{\alpha C}{\pi f}, \tag{1}$$

where C is wave velocity and f is frequency.

For a plane wave propagating in a medium, the amplitude of stress is given by

$$A(L,t) = A_0 e^{-\alpha L} e^{i(kL-\omega t)}, \tag{2}$$

where L is propagation distance, ω is angular frequency, k is wave number, and t is time. Here the $e^{i(kL-\omega t)}$ term represents a propagating wave and the attenuation is determined by the $A_0 e^{-\alpha L}$ term. Let $A(L)$ be $A_0 e^{-\alpha L}$, then α can be calculated from

$$-\frac{d}{dL}\ln A(L) = -\frac{1}{A(L)}\frac{dA(L)}{dL} = \alpha + L\frac{d\alpha}{dL}. \tag{3}$$

From published results specifying the attenuation coefficient [*Gordon and Davis*, 1968; *Brennan and Stacey*, 1977; *Toksoz et al.*, 1979; *Winkler et al.*, 1979; *Johnston et al.*, 1980; *Jackson*, 1993], it can be concluded that $d\alpha/dL = 0$. Then (3) can be written as

$$\alpha = -\frac{d\ln A(L)}{dL}. \tag{4}$$

Two methods can be used to evaluate crack density in rocks, one is suggested by *O'Connell and Budiansky* [1974, 1977] who have established the relation between the crack density and stress wave velocity; the other used by *Grady and Kipp* [1987] and *Rubin and Ahrens* [1991] is the damage parameter defined as

$$D = 1 - \left(\frac{C}{C_0}\right)^2, \tag{5}$$

where C is the wave velocity of the rock with cracks and C_0 is the intrinsic wave velocity of the rock. Because $(C/C_0)^2$ is the ratio of elastic moduli of rocks before and after the damage, D describes the relative modulus change of rocks.

Because stress wave attenuation results from the occurrence of cracks, the relationship between attenuation coefficient and damage parameter has an important role in understanding the propagation of stress waves in damaged rocks. The present study presents the first experimental data describing stress wave attenuation in damaged rocks. Attenuation coefficients and damage parameters (and crack densities) in a series of damaged

Paper number 96JB03891.
0148-0227/97/96JB-03891$09.00

San Marcos gabbro samples were obtained by using the ultrasonic pulse-echo method developed by *Winkler and Plona* [1982].

Experimental Technique

The rock used in this work was San Marcos gabbro (SMG). Shock wave properties and shock effects in SMG have been studied previously [*McQueen et al.*, 1967; *Lange et al.*, 1984; *Polanskey and Ahrens*, 1990; *Rubin and Ahrens*, 1991; *Ahrens and Rubin*, 1993; *He and Ahrens*, 1994]. The density of SMG is 2.87×10^3 kg/m^3, the intrinsic P wave velocity is assumed to be 7.12 km/s (under 0.4 GPa confining pressure)[*Birch*, 1960], and shear velocity is 3.7 km/s (under 0.4 GPa confining pressure) [*Simmons*, 1964]. From the two velocities, the intrinsic shear, bulk and Young's moduli of SMG are 39, 93, and 103 GPa, respectively. The intrinsic Poisson's ratio of SMG is 0.31.

Initially, a SMG target with dimensions 200 × 200 × 150 mm was impacted by a lead projectile at a velocity of 1.2 km/s. The projectile had a diameter of 7 mm and mass of 3 g. The crater shape and fracture details in the target were described by *Ahrens and Rubin* [1993]. The recovered target was cut into 1 cm cubes, such that two surfaces of the samples were paralleled to the impact surface of the target. These cubes were polished until the variation of thickness for each sample was less than 0.03 mm. Because water was used when the samples were polished, the samples were placed in an oven under normal pressure at 100°C for 24 hours before the measurements. This procedure is similar to that used by *Polanskey and Ahrens* [1990].

The pressure of the shock wave induced by the impacting in the target can be estimated using the power decay relation

$$P = P_0\left(\frac{r}{r_0}\right)^{-\beta} \qquad r \geq r_0, \tag{6}$$

where r and r_0 are the radial distance and the equivalent radius of the projectile, respectively. This expression is mainly based on experimental data. P_0 is the shock wave pressure on the impact surface, and β is assumed to be 1.5 for nearly crack-free rocks [*Ahrens and O'Keefe*, 1977]. The initial shock wave pressure P_0 is calculated to be 11 GPa using the impedance-match method [*Ahrens*, 1987] and the equations of state of lead and gabbro [*Ahrens*, 1987; *Ahrens and Johnson*, 1995] and the velocity of projectile. The shock wave pressure in the gabbro target is then estimated as

$$P = 2.27r^{-1.5}, \tag{7}$$

where the unit of P is GPa and r(centimeters) is ≥ 0.35 cm.

From (7) we infer that P decays along the center line of the impact from 11 GPa at a radius of 0.35 cm to about 0.1 GPa at a radius of 8 cm.

The ultrasonic experimental apparatus used in this work is similar to that developed by *Winkler and Plona* [1982] for attenuation coefficient measurements (Figure 1). A positioning screw is used to hold and tighten the whole assembly to insure good contact between the coupling surfaces. The transducer is located along the center line of the assembly.

The thickness of the coupling lucite buffer h_1 is chosen such that the reflecting signals from surfaces A and B can be unambiguously identified. The thickness of the sample is h_2. Also C_{p1} and C_p are P wave velocities for the lucite and sample, respectively. The characteristic times (Figure 1) for the system are

$$t_{p1} = \frac{2h_1}{C_{p1}}, \tag{8}$$

$$t_{p2} = \frac{2h_1}{C_{p1}} + \frac{2h_2}{C_p}, \tag{9}$$

$$t_{p3} = 2t_{p1}. \tag{10}$$

Typical thicknesses and velocities of the buffer and samples are $h_1 = 1$ cm, $h_2 = 1$ cm, $C_{p1} = 2.69$ km/s, and $C_p = 6.5$ km/s. From (8) – (10) we have $t_{p1} = 7.4$ μs, $t_{p2} = 10.5$ μs, and $t_{p3} = 14.8$ μs. From the simple calculation above we conclude that the wave reflected from surface B arrives at the transducer just after the signal from surface A. This ensures that the signals are clearly distinguished.

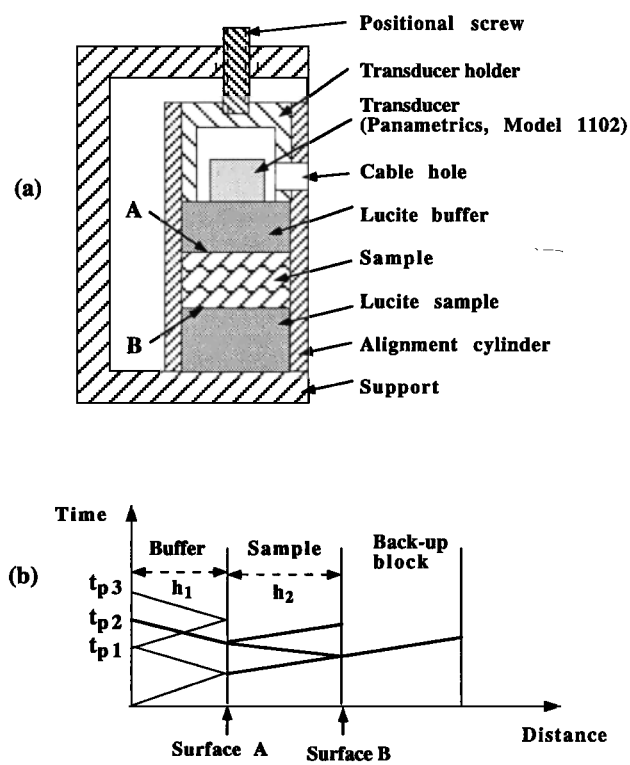

Figure 1. Attenuation measurement system. (a) Sketch of experimental arrangement. (b) Distance and time diagram.

A piezoelectric transducer (Panametrics, Model 1102) is used as the pulse generator and the receiver. The transducer's driver is a Panametrics 5052UA pulser receiver. The ultrasonic signals are recorded using a digital oscilloscope (Gould 4074), and the typical sampling rate used in experiments is 4.9 ns between data points with a signal voltage resolution of 8 bits.

The strain induced by the stress wave in the gabbro sample is measured using a semiconductor strain gauge (Entran, Model ESU-025-1000). It has a gauge factor of 155 and dimensions of 0.64 × 0.13 mm. The strain measurement system is shown in Figure 2. The semiconductor strain gauge is bonded to the surface of the gabbro samples using epoxy (Devcon, TAC 10^{TM}), which solidifies in 24 hours under normal conditions. The signal from the strain gauge is amplified and then recorded using the Gould oscilloscope.

Data Reduction

P wave velocity and damage parameters . P wave velocity is measured by using two transducers. One is an ultrasonic wave generator and the other the receiver. We first measure the time duration for a pulse to be generated and received without an interposing sample between the two transducers. The time duration with the sample is then measured. The propagation time of ultrasonic P waves in each sample is obtained upon subtraction of the two time durations. Further details are described by *Rubin and Ahrens* [1991]. The damage parameter is obtained using the definition of *Grady and Kipp* [1987] (equation (5)).

Attenuation coefficient. The method used in this work is similar to that given by *Winkler and Plona* [1982]. This method is based on the two stress waves reflected from surfaces A and B of the sample, as shown in Figure 1. The stress waves reflected from surface A do not propagate through the sample; the waves reflected from surface B propagate through the sample twice. Because both waves propagate the same distance in the buffer material, the attenuation can be explicitly evaluated.

As in the previous paper [*Winkler and Plona,* 1982] , it is assumed that the reflecting and transmission coefficients of the surfaces between the buffer and the sample are equal to those for plane wave incidence. Thus the change in amplitude with the frequency of the wave results only from attenuation after correction for reflection and transmission of the stress wave at the surfaces.

Suppose that $L/2$ is sample thickness and $A(f)$ and $B(f)$ are the frequency-dependent amplitudes of the pulse reflected from surfaces A and B of the sample, respectively. The attenuation coefficient obtained from these two ultrasonic signals is expressed as [*Winkler and Plona,* 1982]

$$\alpha(f) = \frac{8.686}{L} \ln[\frac{A(f)}{B(f)}(1 - R^2)], \tag{11}$$

where the unit of $\alpha(f)$ is decibels per centimeter when the unit of L is centimeters. The constant results from the change in the attenuation unit (1.0 dB/cm = 8.686 Np/cm). Here R is the reflection coefficient for the interface between the coupling buffer and sample and is given by

$$R = \frac{C_p\rho - C_{pc}\rho_c}{C_p\rho + C_{pc}\rho_c}, \tag{12}$$

where C_p and ρ are the P wave velocity and the density of gabbro samples, respectively. C_{pc} and ρ_c are the P wave velocity and density of the coupling buffer (lucite), respectively. From ultrasonic measurements, C_{pc} is 2.68 km/s and ρ_c is 1.19×10^3 kg/m^3. These data are similar to the results of *Hartmann and Jarzynski* [1972] (C_{pc} = 2.69 km/s and $\rho_c = 1.19\times10^3$ kg/m^3). In the calculation of attenuation coefficients, a possible correction of attenuation due to wave spreading was not

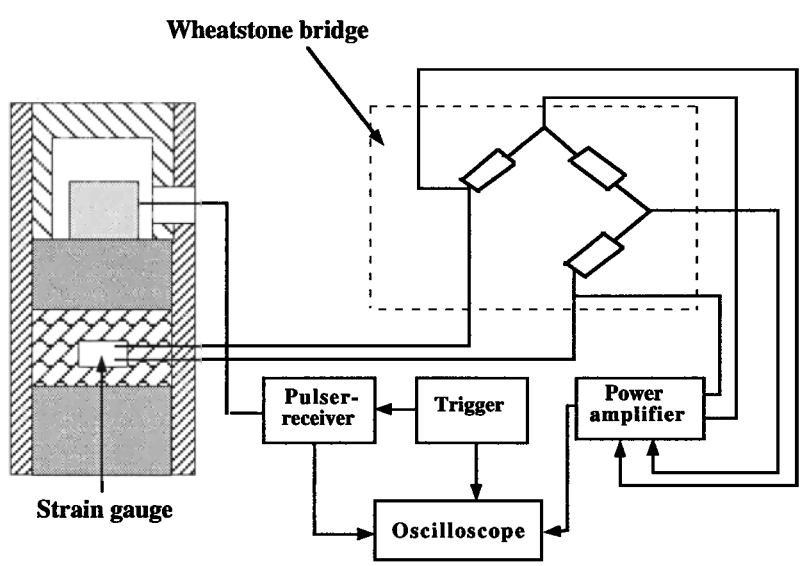

Figure 2. Sketch of the strain measurement arrangement.

considered because we were unable to model explicitly the behavior of rocks with different crack densities.

In order to obtain attenuation coefficients, a fast Fourier transform (FFT) is employed to calculate the frequency spectrum of the two signals. Then the attenuation coefficient versus frequency is obtained using (11). The FFT subroutine used is one of subprograms in the Seismic Analysis Code developed by *Tull* [1989]. There were about 300 – 400 data points in each window. In order to eliminate edge effects, the window was extended to 2048 points by repeating a few points near the boundary of the signal.

Strain measurement . The strain induced by ultrasonic stress waves is measured by the semiconductor strain gauge shown in Figure 2 and is evaluated using

$$e = \frac{\delta R}{\beta R_0}, \tag{13}$$

where β is the gauge factor of the strain gauge and δR and R_0 are the resistance change and the initial resistance of the gauge, respectively.

Because a Wheatstone bridge is used, the relation between the resistance and the voltage change [*Kreuzer*, 1988] is

$$\frac{\delta R}{R_0} = \left(\frac{V_0}{\delta V} - 1\right)^{-1}, \tag{14}$$

where δV and V are the voltage change and the supply voltage across the strain gauge, respectively. The strain amplitude is calculated with (13) and (14).

Experimental Results and Analysis

The P wave velocities and damage parameters for about 20 samples are listed in Table 1 with their positions in the initial target. A typical signal recorded for the attenuation measurement is shown in Figure 3. Typical results of spectral analysis are shown in Figure 4. Using (5) and (11), the attenuation coefficients for the samples with different damage parameters have been evaluated (Table 1). Figure 5 shows the attenuation coefficient dependence versus frequency for samples with different damage parameters from the FFT calculation. From these results, we can see that the attenuation coefficients increase with both frequency and damage parameter.

Figure 6 shows the attenuation coefficient dependence on the damage parameter for the frequency of 2 MHz (the peak energy of the ultrasonic P wave is at $\sim$ 2 MHz). The data are fitted with

$$\alpha_p = 1.1 + 28.2 D_p, \tag{15}$$

where α_p is in decibels per centimeter.

From (1), (5), and (15), the quality factor of the damaged samples is

$$Q^{-1} = 0.011(1 + 25.6 D_p)(1 - D_p)^{1/2}, \tag{16}$$

which is plotted in Figure 7.

Table 1. Experimental Results

X, cm	Y, cm	C_p, km/s	D_p	α_p, dB/cm	Q
4.93	1.89	6.02	0.285	8.2	13.0
4.93	4.36	6.31	0.215	7.3	15.8
4.93	8.20	6.44	0.181	5.2	17.8
7.47	4.36	6.10	0.267	7.9	13.5
3.64	4.36	5.74	0.349	10.5	11.3
7.47	8.20	6.72	0.108	5.0	25.6
7.47	6.82	6.48	0.171	6.7	16.6
3.64	6.82	6.09	0.269	8.8	13.5
2.35	5.58	5.87	0.319	9.4	12.0
3.64	5.58	6.34	0.207	7.5	16.2
8.75	5.58	6.77	0.096	4.4	27.6
6.20	5.58	6.44	0.181	5.2	17.8
7.47	5.58	6.49	0.168	5.7	18.8
4.93	3.12	6.29	0.220	8.4	15.5
6.20	3.12	6.46	0.176	7.2	17.4
7.47	3.12	6.29	0.220	7.7	15.5
8.75	3.12	6.46	0.177	5.9	18.1
3.64	8.20	6.56	0.151	4.6	20.3
8.75	8.20	6.60	0.140	5.0	21.4
3.64	3.12	5.65	0.365	12.0	11.0

The definitions of X and Y are given in Figure 8.

In order to relate the attenuation coefficient to the location of samples in the initial target, a coordinate system is defined in Figure 8. Figure 9 shows the experimental results of attenuation coefficients versus the radius from the impact point. The relation between attenuation coefficient and radial distance is found to be

$$\alpha_p = 48.9 r^{-0.95}, \tag{17}$$

where r(centimeters) is radial distance. Thus, as expected, the attenuation coefficients of the samples decrease with increasing distances from the impact point. It must be noted that only the attenuation coefficients along direction X (Figure 8) are measured because we

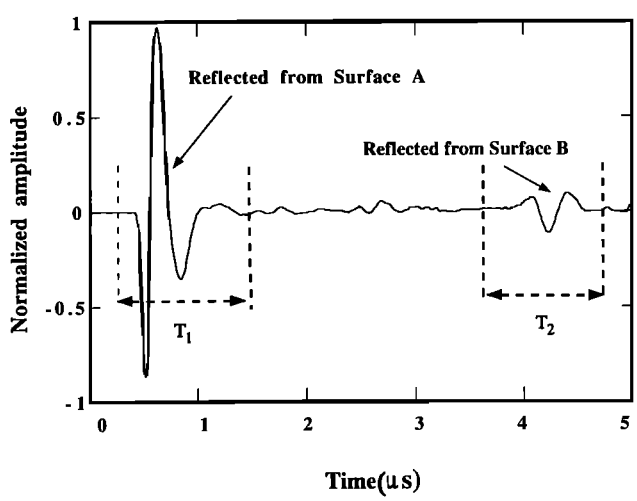

Figure 3. Typical ultrasonic record. T_1 and T_2 are the data periods (used in FFT) of the signals reflected from surface A and surface B, respectively.

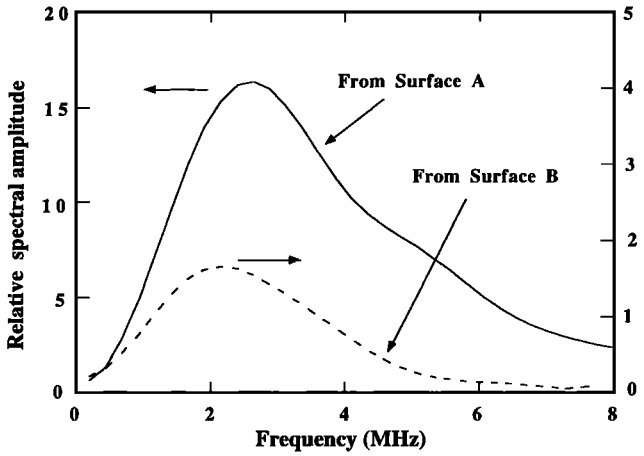

Figure 4. Typical spectral amplitude of signals.

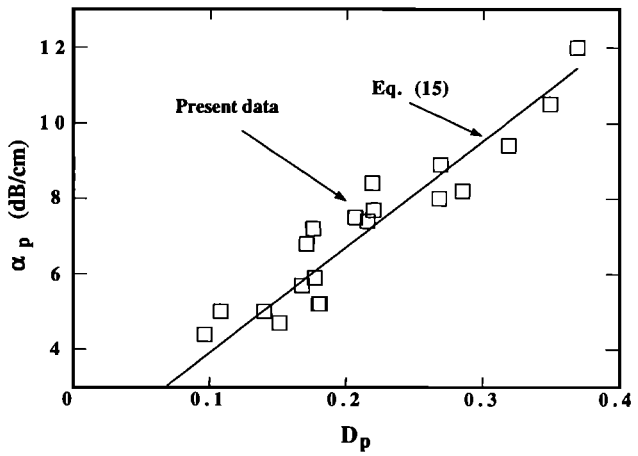

Figure 6. Relation between damage deficit and attenuation coefficient.

are mainly interested in the relation between attenuation coefficients and damage parameters. In general, the damage in samples induced by shock waves is anisotropic. This will of course result in anisotropy in the attenuation of shock-damaged samples. In order to investigate attenuation anisotropy, additional measurements are required. This may be a direction of future research.

Figure 10 demonstrates that the largest strain in the SMG samples induced by ultrasonic waves is about 2×10^{-7} (The sample used in this measurement was undamaged SMG.). We note that the shape of the strain gauge signal is dissimilar to that recorded by the piezoelectric transducer in Figure 3. The main reason for this is that the time resolution of the semiconductor strain gauge is poorer than that of the piezoelectric transducer because of the strain gauge's large dimensions. However, the strain amplitude can be used to approximately evaluate the strain induced in the samples.

For dry circular cracks, *O'Connell and Budiansky* [1974] have established the relation between P wave velocities, C_p (damaged samples) and C_{p0} (intrinsic velocity), and crack density as

$$\left(\frac{C_p}{C_{p0}}\right)^2 = \frac{(1-\nu)(1+\nu_0)K}{(1+\nu)(1-\nu_0)K_0}, \tag{18}$$

$$\frac{K}{K_0} = 1 - \frac{16(1-\nu^2)\varepsilon}{9(1-2\nu)}, \tag{19}$$

$$\frac{\nu}{\nu_0} = 1 - \frac{16\varepsilon}{9}, \tag{20}$$

where ν and ν_0 are the effective and the intrinsic Poisson's ratio, respectively, and K and K_0 are the effective and the intrinsic bulk moduli, respectively. The crack density is defined as

$$\varepsilon = N < a^3 >, \tag{21}$$

where N is the number of cracks per unit volume and a is the half-length of cracks.

O'Connell and Budiansky's relations are derived for penny-shaped, circular cracks. Although cracks in shock-damaged rocks are not circular in detail, we adopt their

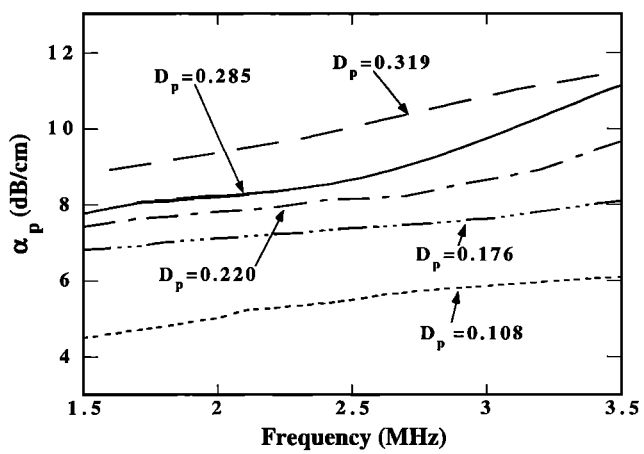

Figure 5. Experimental results of attenuation coefficient versus frequency for the samples with different damage parameters.

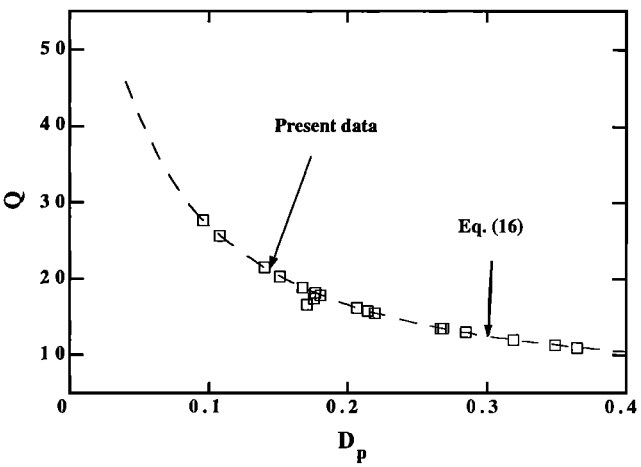

Figure 7. Quality factor versus damage parameter.

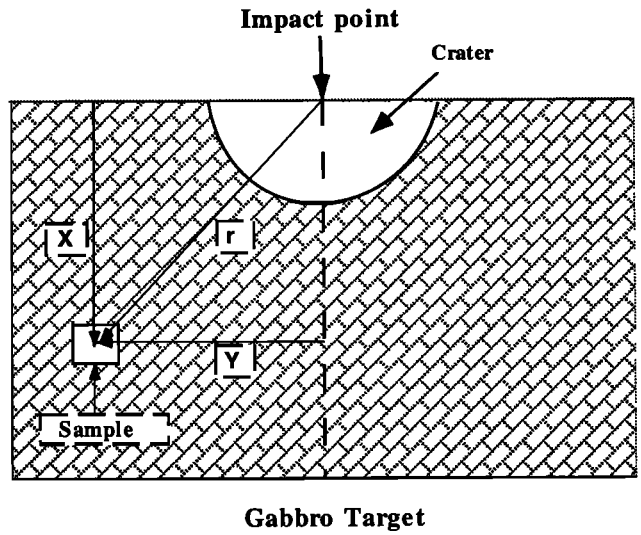

Figure 8. The definition of coordinate system relative to impact point and crater.

equations and assume that their equations are good approximations to the present damaged samples. Moreover, in the present paper, the strain and strain rate of the ultrasonic waves in the samples are low, and although *O'Connell and Budiansky*'s theory is for "static" moduli, we believe that it applies in the present case. The damage parameter is then written as

$$D_p = 1 - \left(\frac{C_p}{C_{p0}}\right)^2 = 1 - \frac{(1-\nu)(1+\nu_0)K}{(1+\nu)(1-\nu_0)K_0}, \quad (22)$$

and upon substituting (19) and (20) into (22), the expression for D_p is

$$D_p = 1 - \frac{1+\frac{16\nu_0\varepsilon}{9(1-\nu_0)}}{1-\frac{16\nu_0\varepsilon}{9(1+\nu_0)}}\left[1 - \frac{16(1-\nu_0{}^2(1-\frac{16\varepsilon}{9})^2)}{9(1-2\nu_0(1-\frac{16\varepsilon}{9}))}\varepsilon\right]. \quad (23)$$

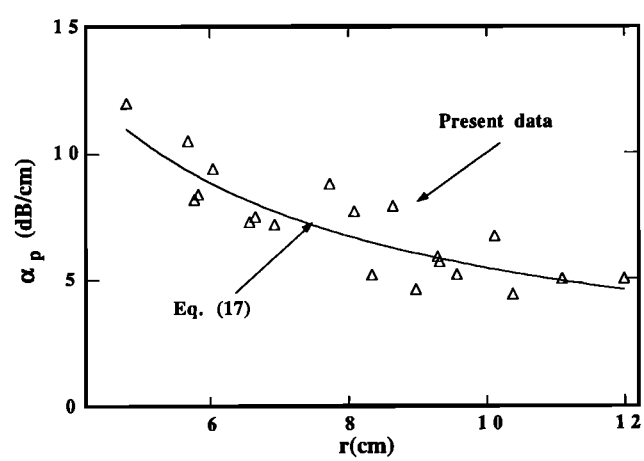

Figure 9. The relation between attenuation coefficient and radial distance.

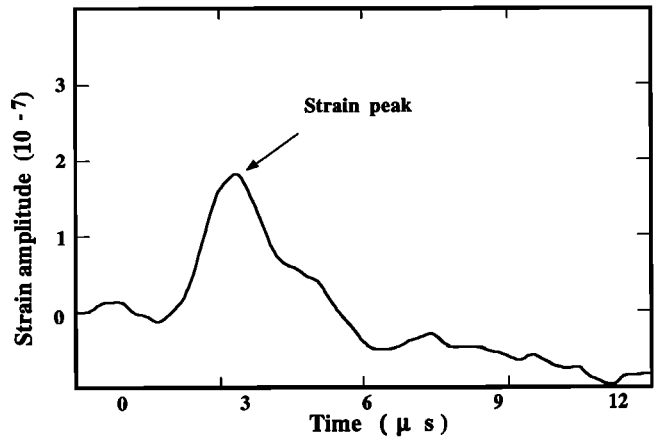

Figure 10. Typical strain profile.

Since ν_0 is known, ε versus D_p can be calculated from (23). The relation between D_p and ε can be fit by the equation

$$D_p = 2.4\varepsilon - 1.2\varepsilon^2. \quad (24)$$

From (15) and (24) we obtained an approximate expression relating α to ε,

$$\alpha_p = 1.1 + 67.7\varepsilon(1 - 0.5\varepsilon). \quad (25)$$

Figure 11 presents the experimental results of attenuation versus crack density and the calculated results from the expressions above (crack density is calculated by solving (24) for D_p).

Walsh[1966] gave an expression for the P wave quality factor Q as

$$Q^{-1} = \frac{E}{E_0}\frac{(1-\nu)}{(1-2\nu)}\varepsilon F(\mu,\nu), \quad (26)$$

where Q^{-1} is the reciprocal of the quality factor and E and E_0 are the effective and intrinsic Young's moduli, respectively. $F(\mu,\nu)$ is the function of the internal friction coefficient μ and the effective Possion's ratio ν.

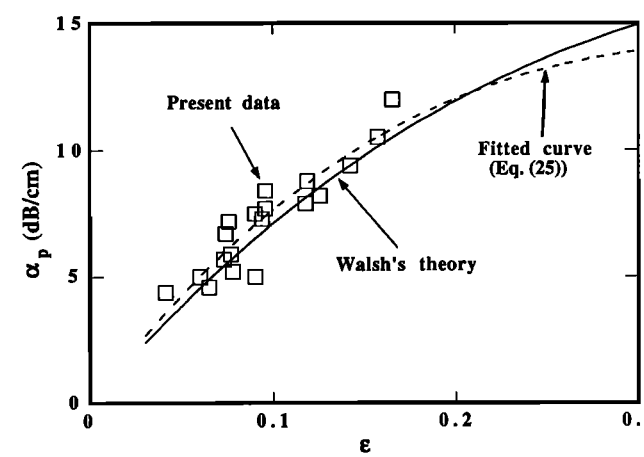

Figure 11. The relation between attenuation coefficient and crack density.

For simplicity we assume that $F(\mu,\nu)$ is approximately a constant for a given material. Then, from the relation between E and K, the expression for the quality factor is

$$Q^{-1} = F\varepsilon\frac{K(1-\nu)}{K_0(1-2\nu_0)}, \tag{27}$$

and from (19), (20), and (27), $Q^{-1}(\varepsilon)$ can be calculated provided the parameter F is determined.

Based on the experimental results for the quality factor and (19), (20), and (27), F is found to be 0.55 ± 0.05 (for each datum, Q and ε are known and F was determined using (27)). Comparisons of attenuation coefficients and quality factors between the experimental results (Table 1), (15) and (16) and Walsh's theory (equation (27)) are shown in Figures 11 and 12. The calculated result from Walsh's theory is in good agreement with the experimental results upon the fitting of F, although the relation between Q or α and ε is nonlinear.

Because attenuation coefficients depend on the surface area of cracks, the change of attenuation coefficients with damage level reflects the change of crack surface area; therefore the average crack size can be estimated from the attenuation coefficient. If we assume approximately that the attenuation coefficient depends linearly on the average crack surface area, that is, $\alpha_p \propto a^2$ (a is the average half-length of cracks), and that the crack density is proportional to the average volume of cracks, that is, $\varepsilon \propto a^3$, the average half-length of cracks can be written as

$$a = \frac{h\varepsilon}{\alpha_p}, \tag{28}$$

where h is an undetermined constant.

From the data for SMG given by *Ahrens and Rubin*[1993] ($\varepsilon = 0.01$ when $a \approx 0.4$ mm) and (25), h is determined to be 7.1 dB. The average half-length of cracks is

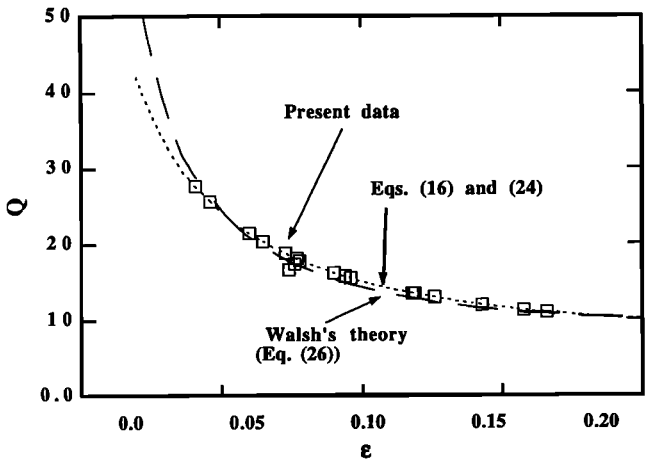

Figure 12. Quality factor versus crack density.

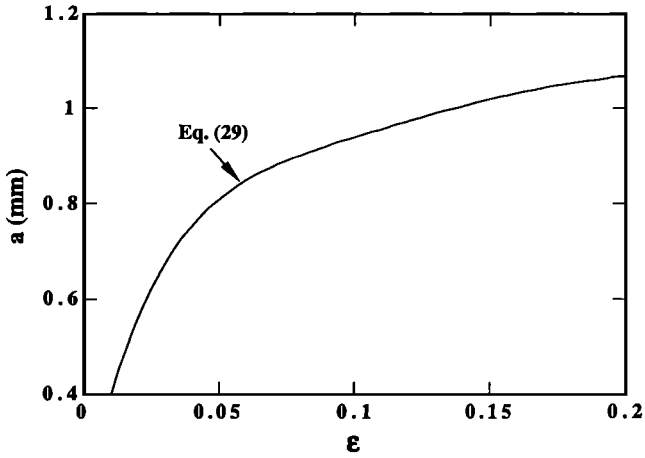

Figure 13. Average half-length of cracks versus crack density.

$$a = \frac{7.1\varepsilon}{1.1 + 67.7\varepsilon(1-0.5\varepsilon)}, \tag{29}$$

where a is in centimeters. The calculated values of a as a function of ε are shown in Figure 13.

Conclusions

Some 20 samples of San Marcos gabbro were cut from a target in which the in situ P wave velocity varies from 5.65 to 6.77 km/s at radii of 5 to 11 cm from the impact site. The shock wave pressure varies from about 2 GPa at 5 cm to 0.6 kbar at 11 cm. The attenuation coefficients of the samples are measured using ultrasonic methods. We also measure the strain induced by the ultrasonic stress wave using semiconductor strain gauges. We use *O'Connell and Budiansky's* [1974] theory to evaluate the crack density versus the damage parameter. *Walsh's* [1966] theory is used to calculate the quality factor and attenuation coefficient versus the damage parameter. The main results obtained in this work are given,

1. We obtain a relation (equation (15)) between the P wave attenuation coefficient and damage parameter.
2. The relationship (equation (16)) between quality factor and damage parameter is obtained based on the experimental results.
3. Based on *O'Connell and Budiansky's* theory, the relation between the crack density and damage parameter can be expressed approximately as (24).
4. The relation between attenuation coefficients and the radius from the impact point is given (equation (17)).
5. The parameter in the expression (equation (27)) given by Walsh is determined approximately. Walsh's theory on the attenuation coefficient is in good agreement with the experimental data.
6. The average half-length of cracks is approximately estimated from the attenuation coefficient (equation (29)).

7. Using semiconductor strain gauges, the strain induced in the sample by the ultrasonic stress wave was measured to be about 2×10^{-7}.

Acknowledgments. We thank T. Duffy, T. Mukerji, and D. R. Schmitt for numerous suggestions that improved the manuscript, and we thank G. Ravichandran for the use of the ultrasonic apparatus. This research was supported by NASA under NAGW-1941 and Air Force Technical Application Center, Contr. F19628-95-c-0115. Contribution 5631, Division of Geological and Planetary Sciences, California Institute of Technology.

References

Ahrens, T. J., Shock wave techniques for geophysics and planetary physics, in *Methods of Experimental Physics*, edited by C. G. Sammis and T. L. Henyey, vol. 24, pp. 185–235, Academic, San Diego, Calif., 1987.

Ahrens, T. J., and M. L. Johnson, Shock wave data for rocks, in *Rock Physics and Phase Relations: A Handbook of Physical Constants, AGU Ref. Shelf Ser.*, vol.3, edited by T. J. Ahrens, pp. 35–44, AGU, Washington, D. C., 1995.

Ahrens, T. J., and J. D. O'Keefe, Equations of state and impact-induced shock-wave attenuation on the moon, in *Impact and Explosion Cratering*, edited by D. J. Roddy, R. O. Pepin, and R. B. Merrill, pp. 639–656, Pergamon, Tarrytown, N. Y., , 1977.

Ahrens, T. J., and A. L. Rubin, Impact-induced tensional failure in rock, *J. Geophys. Res., 98,* 1185–1203, 1993.

Birch, F., The velocity of compressional waves in rocks to 10 kilobars, *J. Geophys. Res., 65,* 1083–1102, 1960.

Born, W. T., The attenuation constant of Earth materials, *Geophysics, 6,* 132–148, 1941.

Brennan, B. J., and F. D. Stacey, Frequency dependence of elasticity of rock–test of seismic velocity dispersion, *Nature, 268,* 220–222, 1977.

Gladwin, M. T., and F. D. Stacey, Anelastic degradation of acoustic pulses in rocks, *Phys. Earth Planet. Inter., 8,* 332–334, 1974.

Gordon, R. B., and L. A. Davis, Velocity and attenuation of seismic waves in imperfectly elastic rock, *J. Geophys. Res., 73,* 3917–3935, 1968.

Grady, D. E., and M. E. Kipp, Dynamic rock fragmentation, in *Fracture of Mechanics of Rock*, edited by B. K. Atkinson, pp. 429–475, Academic, San Diego, Calif., 1987.

Hartmann, B., and J. Jarzynski, Ultrasonic hysteresis absorption in polymers, *J. Appl. Phys., 43,* 4303–4312, 1972.

He, H., and T. J. Ahrens, Mechanical properties of shock-damaged rocks, *Int. J. Rock Mech. Min. Sci. Geomech. Abstr., 31,* 525–533, 1994.

Jackson, I., Progress in the experimental study of seismic wave attenuation, *Annu. Rev. Earth Planet. Sci., 21,* 375–406, 1993.

Johnston, D. H., and M. N. Toksoz, Ultrasonic *P* and *S* wave attenuation in dry and saturated rocks under pressure, *J. Geophys. Res., 85,* 925–936, 1980.

Johnston, D. H., M. N. Toksoz, and A. Timur, Attenuation of seismic waves in dry and saturated rocks: Theoretical models and mechanisms, *J. Geophys., 44,* 691–711, 1978.

Kreuzer, M., Linearity and sensitivity error in the use of single strain gauge with voltage-fed and current-fed circuits, *Strain Gauge Transducer Tech., 1,* 10–15, 1988.

Lange, M. A., T. J. Ahrens, and M. B. Boslough, Impact cratering and spall fracture of gabbro, *Icarus, 58,* 383–395, 1984.

McQueen, R. J., S. P. Marsh, and J. N. Fritz, Hugoniot equation of state of twelve rocks, *J. Geophys. Res., 72,* 4999–5036, 1967.

Murphy, W. F., Acoustic measures of partial gas saturation in tight sandstones, *J. Geophys. Res., 89,* 11549–11559, 1984.

Nur, A., and G. Simmons, The effect of viscosity of a fluid phase on velocity in low porosity rocks, *Earth Planet. Sci. Lett., 7,* 99–108, 1969.

O'Connell, R. J., and B. Budiansky, Seismic velocities in dry and saturated cracked solids, *J. Geophys. Res., 79,* 5412–5426, 1974.

O'Connell, R. J., and B. Budiansky, Viscoelastic properties of fluid saturated cracked solids, *J. Geophys. Res., 82,* 5719–5735, 1977.

Papadakis, E. P., K. A. Fowler, and L. C. Lynnworth, Ultrasonic attenuation by spectrum analysis of pulses in buffer rods, *J. Acoust. Soc. Am., 53,* 1336–1341, 1973.

Polanskey, C., and T. J. Ahrens, Impact spallation experiments: Fracture patterns and spall velocities, *Icarus, 87,* 140–155, 1990.

Rubin, A. M., and T. J. Ahrens, Dynamic tensile failure induced velocity deficits in rock, *Geophys. Res. Lett., 18,* 219–223, 1991.

Simmons, G., Velocity of shear waves in rocks to 10 kilobars, *J. Geophys. Res., 69,* 1123–1130, 1964.

Spetzler, H., and D. L. Anderson, The effect of temperature and partial melting on velocity and attenuation in a simple binary system, *J. Geophys. Res., 73,* 6051–6060, 1968.

Toksoz, M. N., D. H. Johnston, and A. Timur, Attenuation of seismic waves in dry and saturated rocks: Laboratory measurements, *Geophysics, 44,* 681–690, 1979.

Tull, J. E., *Manual for the Seismic Analysis Code,* Univ. of Calif. Press, Berkeley, 1989.

Walsh, J. B., Seismic wave attenuation in rock due to friction, *J. Geophys. Res., 71,* 2591–2599, 1966.

Winkler, K. W., and A. Nur, Seismic attenuation: Effects of pore fluids and frictional sliding, *Geophysics, 47,* 1–15, 1982.

Winkler, K. W., and T. J. Plona, Technique for measuring ultrasonic velocity and attenuation spectra in rocks under pressure, *J. Geophys. Res., 87,* 10,776–10,780, 1982.

Winkler, K. W., A. Nur, and M. Gladwin, Friction and seismic attenuation in rocks, *Nature, 227,* 528–531, 1979.

T. J. Ahrens and C. Liu, Lindhurst Laboratory of Experimental Geophysics, Seismological Laboratory, 252-21, California Institute of Technology, Pasadena, CA 91125. (e-mail: tja@caltech.edu; liu@seismo.gps.caltech.edu)

(Received January 3, 1996; revised December 10, 1996; accepted December 11, 1996.)